Harmonic Analysis of Electromagnetic Torque in Brushless Direct Current Motors

Monica Adela Enache, Ion Vlad and Sorin Enache

Faculty of Electrical Engineering, Univesity of Craiova, Romania
senache@em.ucv.ro, menache@em.ucv.ro

Abstract – **This study has aimed at establishing and analyzing the causes that produce oscillations of electromagnetic torque developed by brushless direct current motor. The study opportunity is given by the progresses obtained in command and power electronics, which made this motor performant from technical and economic viewpoint. The specialty literature reveals that important torque oscillations occur in this motor in a complete rotation. That is why, this study and the simulations presented here emphasize that there are five classes of slots relatively to the torque magnitude developed and the fact that all the slots are active, that meaning that the average torque developed occurs in the rotation direction. The harmonic analysis reveals that the torque distortion, within the five classes of slots, is variable between 51.03% and 97.63%. The torques computed for the slots classes are between the minimum limit of 0.029 Nm and the maximum one of 0.077 Nm. The low speed torque oscillations can be reduced with a high inertia moment, a speed reaction loop and a performant control system. The importance of the research theme is justified by what we have presented before and is a subject of major interest for engineering.**

Cuvinte cheie: *motor de curent continuu fara perii, design, cuplu electromagnetic, oscilatii de cuplu.*

Keywords: *brushless direct current motor, design, electromagnetic torque, torque oscillations.*

I. IMPORTANCE OF DRIVING LIGHT VEHICLES WITH BRUSHLESS DIRECT CURRENT MOTORS

Electrical devices and installation supplied by local energy sources use permanent-magnet direct current motors, generally brushless motors. Such motors are also experienced in high-power drives: rolling mills, electrical cars and trucks [1-4].

These motors performances have increased by research, which has found new electro-technical materials and by developing the command and power electronics, which increased the conversion of the battery energy.

Brushless direct current motors are generally used for driving light vehicles: electrical bicycle, Fig. 1.a, [5], electrical motor scooter, Fig. 1.b, [6], electrical tricycle, Fig. 1.c, [7], trolleys for disabled, Fig. 1.d, [8].

In case of these vehicles (bicycle/motor scooter/tricycle/electrical trolley), the constructive solution adopted is closed, IP 44, and the motor is placed even in the wheel hub.

The constructive solution is with inner stator, made of steel sheets, with slots, where the winding is placed. The rotor is an outer one, made of steel, shaped as a cylinder, and there are inner permanent magnets, stuck, shaped as a parallelepiped.

Fig. 1. Electrically driven light vehicles for people transport: a) bicycle; b) motor scooter c) tricycle d) trolley for disabled people.

In order to have high operation performances, rare-earth based permanent magnets are used, [9-13]. Load operation means motor heating, because of the losses occurring inside the machine.

High currents and temperatures contribute to demagnetization. That is why, the drives that use brushless direct current motors and must be correctly designed.

The problem of the demagnetization caused by the load current is not considered because the current is permanently controlled and it is limited by the controller and the heating is verified by measuring the temperature.

This paper aims at identifying the causes which produce electromagnetic torque oscillations and at limiting these oscillations [14-18].

II. MODELLING AIR-GAP MAGNETIC FIELDS

The study is made with a brushless direct current motor having 2p=30 –number of poles, N_{cr}=27 –number of slots, Fig.2. The notations are as follows: β - command angle of the current in the phase *a*, α - geometrical angle of rotor displacement, γ -delay angle for the control of the current

I_a. Case $\alpha = 0$, when the axis of the slot "1" passes through O. Thus, the following relations results:

$$\beta = p \cdot \alpha + \gamma \qquad (1)$$
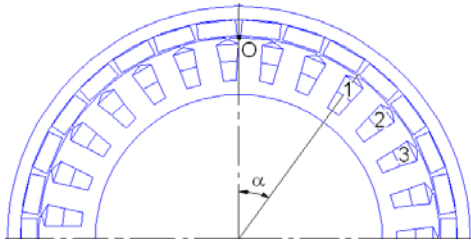
Fig.2. Cross section through the motor.

If the slot opening is neglected, the armature can be considered as being smooth and, in these circumstances, the inductor magnetic field is modelled as a curvilinear trapeze on the entire magnet width. The field is zero on the distance between two successive magnets.

Based on these considerations, the air-gap magnitude has been modelled, Fig. 3, relatively to x [mm] coordinate or to α [°]. Thus, the air-gap magnetic induction curve has resulted relatively to the rotor position, Fig. 4:

$$B = f(\alpha) \qquad (2)$$
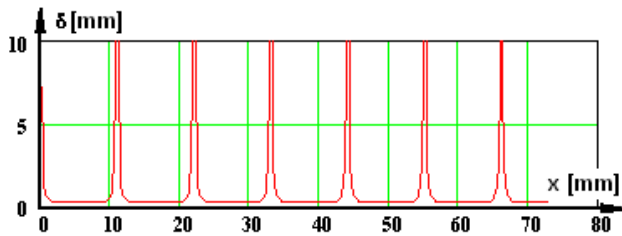
Fig.3. Curve modelling the air-gap magnitude.
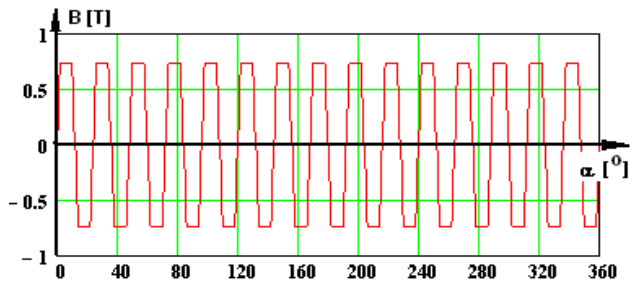
Fig.4. Distribution curve of the air-gap magnetic induction on the entire machine.

On the stator there is a star-connection three-phase winding, no null wire and two series connected phases during the operation. The winding is made in double layer, with coils concentrated on teeth, being a basic constructive component, which condition machine energetic parameters and cost.

The alternating stator currents are trapezoidal shaped, the duration of one pulse being of 120 electrical degrees. For $\alpha = 0$ the armature ampere-turn curve has been computed and plotted, Fig. 5.a, considering the ampere-turn concentrated in the slot axis.

Because it is a much distorted quantity, the harmonic analysis of the curve has been made, Fig. 5.b, the distortion factor has been computed, $k_{dis} = 98.6\%$, and a big number of important harmonics has been emphasized.

It is noticed that the 15-th order harmonic (which is not the most important one in terms of magnitude, Fig.5.a), accomplishes the condition of equality of the poles number on the two armatures (2p=30).
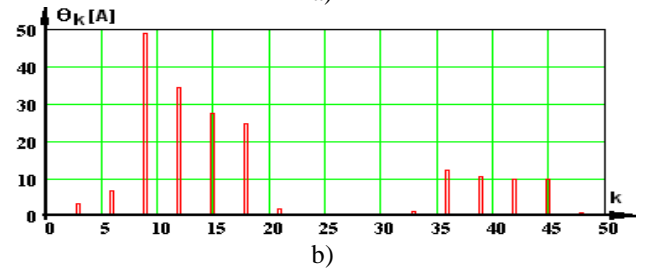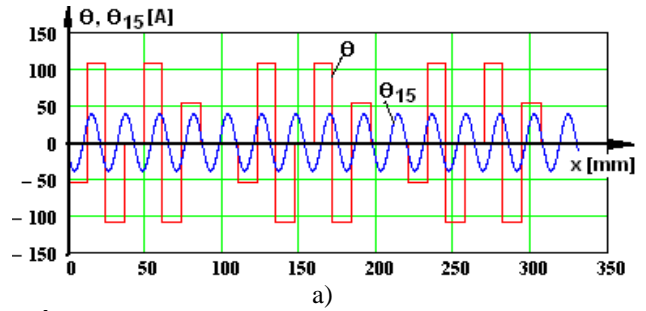
Fig.5. Armature reaction ampere-turn: a) curve and the 15-th order harmonic b) harmonic spectrum.

The air-gap dimension was numerically modelled at establishing the inductor magnetic field, so the curve of the reaction filed and the curve of the resultant field can be plotted, Fig.6.
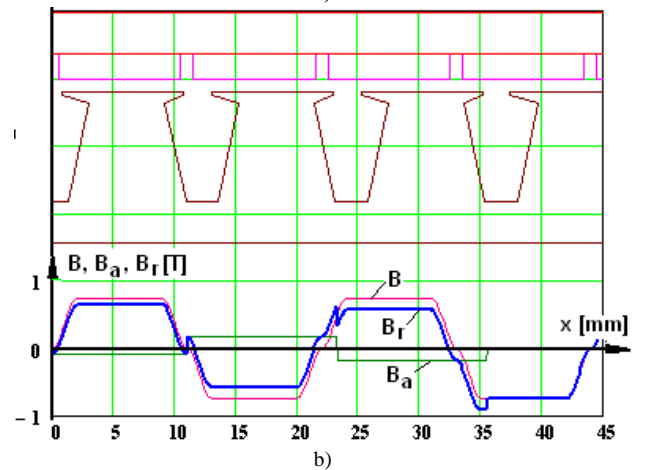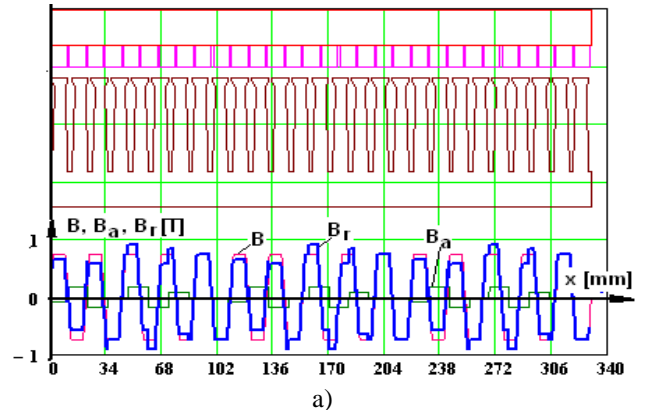
Fig.6. Plan section through the analyzed motor and the curves of the magnetic fields, B –inductor , B_a –reaction, B_r –resultant for: a) entire machine; b) on two pole pairs.

If the time origin t=0 is considered when α= 0, the numerical modelling of currents results relatively to the rotor position and the currents control:

$$I_a, I_b, I_c = f(\alpha, \gamma) \qquad (3)$$

The control device models, on a pole pair, the currents of the three phases of the winding relatively to β - electrical angle, dependent on the rotor position. For the slot N_{cx}, the geometrical angle is:

$$\zeta_{Ncx} = \alpha + \frac{360}{N_c} N_{cx} \qquad (4)$$

The ampere-turn provided by a slot is:

$$\theta_{Ncx} = 0.5 \cdot n_c (I_x + I_y) \qquad (5)$$

where, n_c –number of conductors/slot, I_x, I_y are the currents I_a, I_b or I_c, relatively to the slot distribution on zones and phases, made according to literature.

In most cases, it is considered that the ampere-turn of a slot is concentrated in its axis and at the air-gap level.

This way, a numerical modelling of the slots electromagnetic torques has been established, as follows:

$$M_{Ncx} = B(\alpha) \cdot \theta_{Ncx}(\alpha, \gamma, N_{cx}) \cdot l_{Fe} \qquad (6)$$

The instantaneous value of the electromagnetic torque results by summing the elementary torques of the slots.

The research can be carried on by using a program which is based on the presented mathematical model. There will be noted $N_{p\alpha}$ –number of points for a complete rotation and $N_{p\gamma}$ –number of points in which the control is delayed, for a pole pair. Thus, the following angles result:

$$\alpha_e = k_{p\alpha} \frac{360}{N_{p\alpha}} \qquad k_{p\alpha} = 1,2,3..., N_{p\alpha} \qquad (7)$$

$$\gamma_e = k_{p\gamma} \frac{360}{N_{p\gamma}} \qquad k_{p\gamma} = 1,2,3..., N_{p\gamma} \qquad (8)$$

For all combinations of values α_e, γ_e which result, there are computed and memorized the instantaneous values and the average value of the torque provided by a slot, respectively the total average torque, for a complete rotation.

III. SIMULATIONS AND RESULTS OBTAINED

The mathematical model presented was the basis of a numerical computation program and the simulations carried out and their results obtained enable identifying the causes and establishing important conclusions regarding the electromagnetic torque pulsations in brushless direct current motor.

From economic and technical considerations, there have been identified the following four possibilities for the motor supply:

Six-pulse supply for a pole pair

   -normal sequence of phases

   -inverse sequence of phases

Three-pulse supply for a pole pair

   - normal sequence of phases

   - inverse sequence of phases

In case of six-pulse supply and normal sequence of phases, the electromagnetic torque average value, for a complete rotation and different control angles, is presented in Fig. 7.
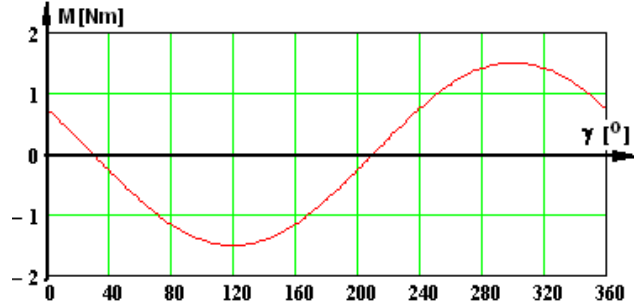
Fig.7. Electromagnetic torque average value in a complete rotation for different control angles of currents.

A. Control for the maximum total torque

From the analysis of this figure, it is noticeable that for γ=294º electrical angle, we have a positive maximum torque (for rotation sense to right) and for γ=114º electrical angle, we have negative maximum value (for rotation sense to left).

The maximum torques have equal absolute values, M_{max}=1.52 Nm. For the electrical angle γ=294º, the geometrical angle results ξ=294/15=19.6º, which shows where the first position transducer must be placed, relatively to the origin – point O, on the stationary armature. The other two position transducers are placed at each 120º electrical angle, in the rotation direction.

The average values, for a complete rotation, of the torques provided by each slot, are presented in Fig. 8 and Fig. 9.a shows the total torque curve, for a complete rotation of the motor. This curve is analyzed from harmonic viewpoint and a harmonic spectrum results in Fig. 9.c, where the important harmonics can be identified, which affect the torque curve, Fig. 9.b.
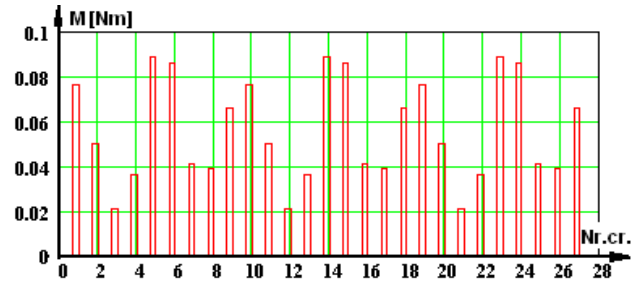
Fig.8. Average values of torques provided by the machine slots for control angle γ=294º M_{Nmed}=1.52 Nm.

a)
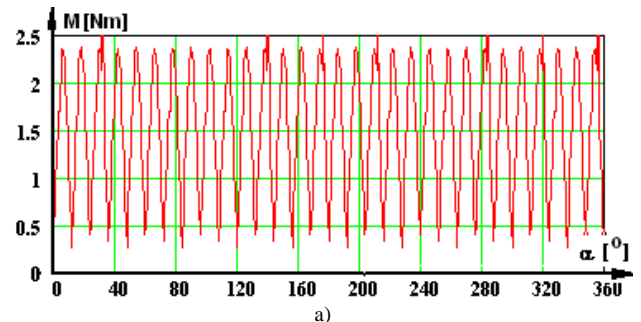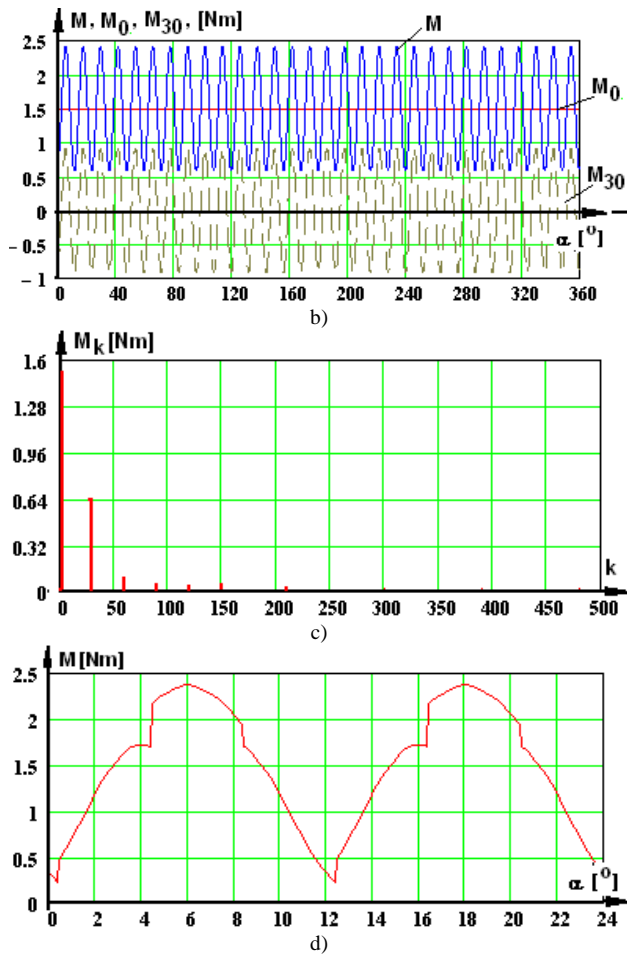
Fig.9. Variation curve of the motor torque: a) for a complete rotation; b) the continuous component and the main harmonic; c) harmonic spectrum; d) torque curve for a pole pair.

The total torque curve for a pole pair is depicted in Fig. 9.d and the harmonic analysis results are filled in the Table I, where there is comparison with the previous results.

B. Analysis of electromagnetic field in each slot

Further on in this paper, a detailed analysis of Fig. 8 is made, in order to divide up in classes the 27 slots of the motor, relatively to the produced average torque. The results of this classification are filled in the Table II.

TABLE I. Analysis of the total torque

	Total torque		Distortion factor
	Average value M_{med} [Nm]	Important harmonics M_k [Nm]	K_{dis} [%]
Analysis for a complete rotation	1.497	M_{30}=0.646 M_{60}=0.069	40.21
Analysis for a pole pair	1.487	M_2=0.655 M_4=0.081	41.06

TABLE II. Slots divided up into classes

Class	Afferent slots	Torque average value
I	5, 6, 14, 15, 23, 24	M_{cr}=0.084 Nm
II	1, 10, 14	M_{cr}=0.077 Nm
III	2, 11, 19	M_{cr}=0.051 Nm
IV	4, 8, 13, 22	M_{cr}=0.038 Nm
V	3, 12, 21	M_{cr}=0.021 Nm

A slot is chosen for each class, the torque curves for a pole pair are presented, Fig. 10, and an analysis is made, from harmonic point of view, Fig. 11.

Any problems occur in the slots 3, 12, 21, where we see large positive and negative torque oscillations (Fig.10.c); in the slots 2, 11, 19 the oscillations are lower (Fig.10.b).

These oscillations cause superior torque harmonics which may exceed even the continuous component, Fig. 11.b and Fig. 11.c, an undesirable effect.

For the analyzed slots, in Fig. 12 there are depicted torque curves, where we have the continuous component, the important harmonic and the resultant torque. The final results of this analysis are detailed in table no. 3, where the distortion factor is also presented.

a) torque provided by the slot no.1

b) torque for the slot no. 2

c) torque for the slot no. 3

d) torque for the slot no. 4

e) torque provided by thr slot no.5

e) torque harmonics for the slot no.5
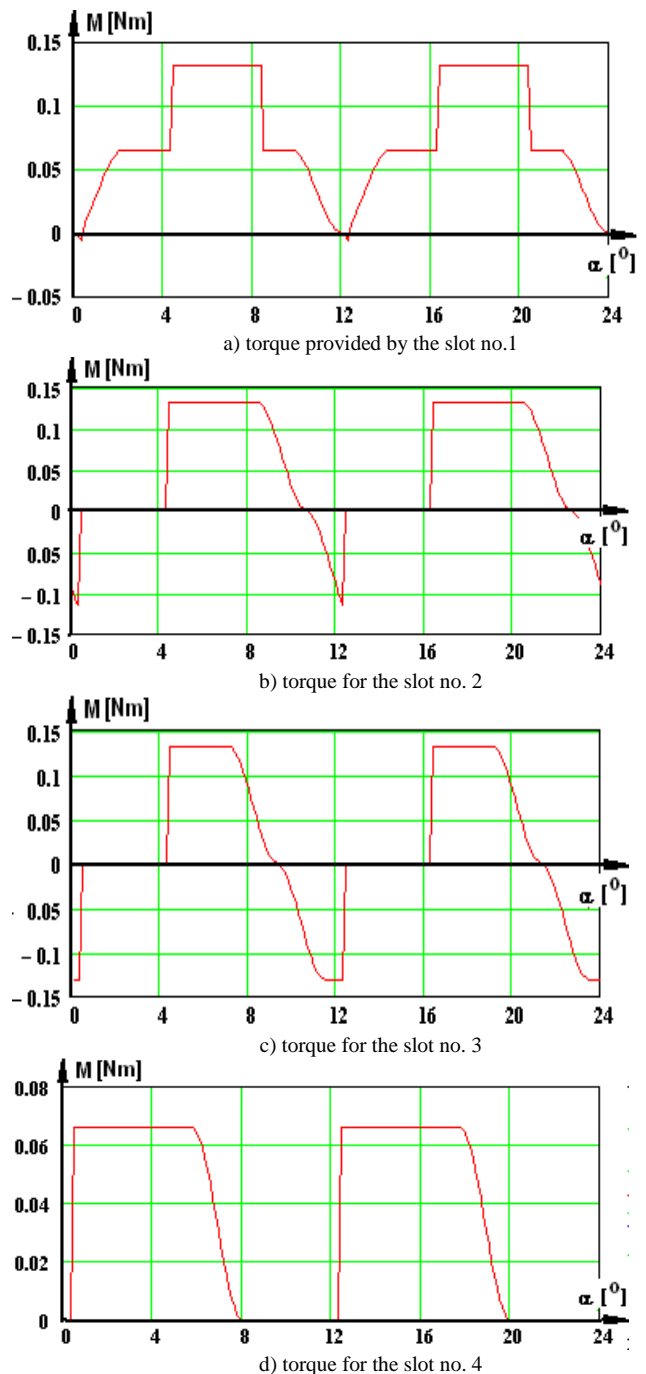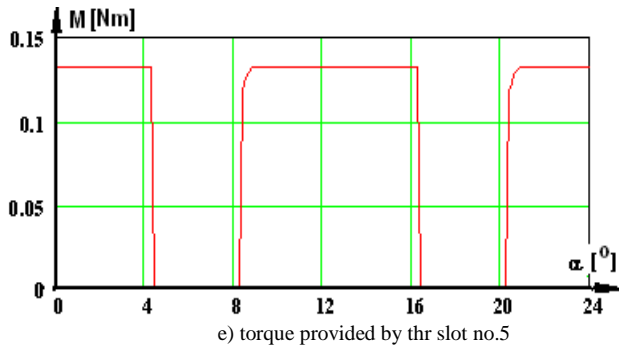
Fig.10. Variation curves for a pole pair for the torque provided by the currents passing the conductors of a slot.
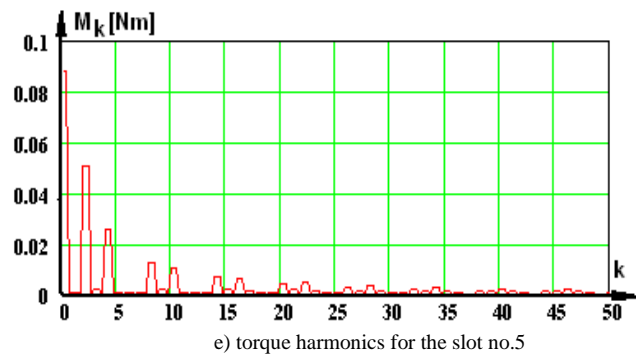
Fig.11. Harmonic spectrum for the torque curves presented in fig.5.

a) torque harmonics in the slot no. 1

a) slot no. 1

b) torque harmonics for the slot no. 2

b) slot no. 2

c) torque harmonic in the slot no.3

c) slot no. 3

d) torque harmonics for the slot no. 4
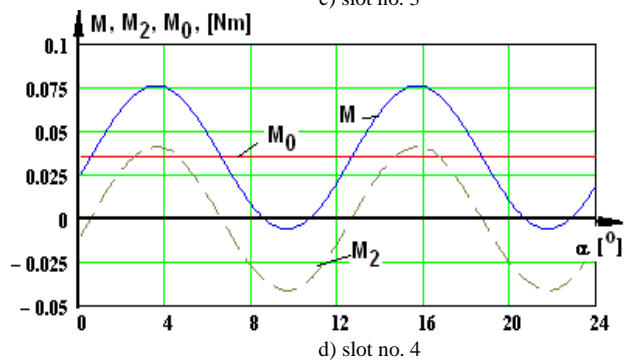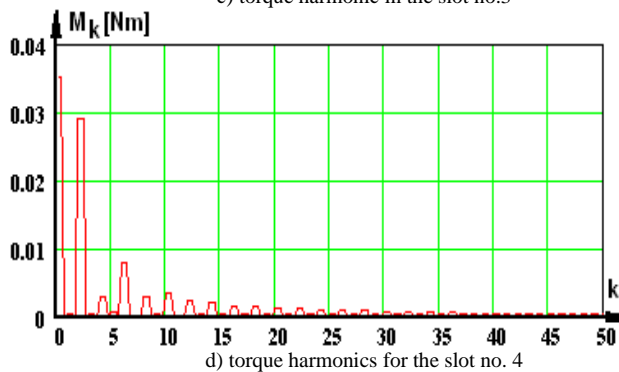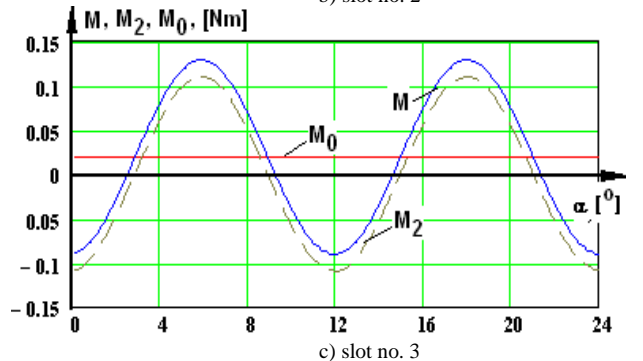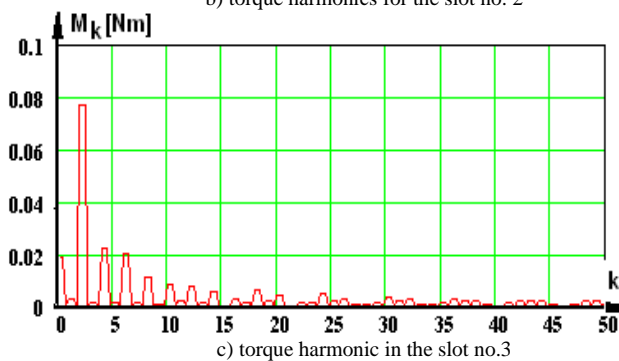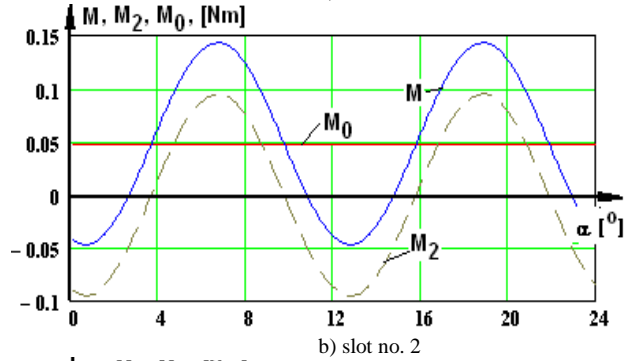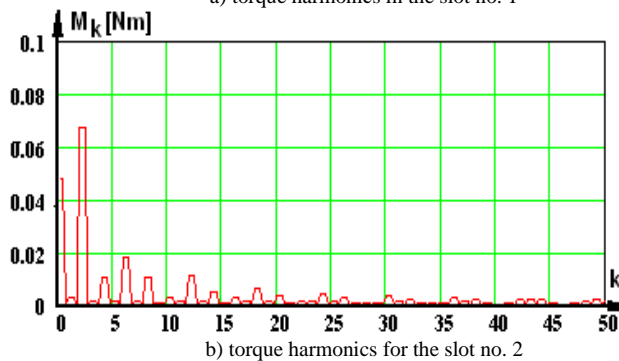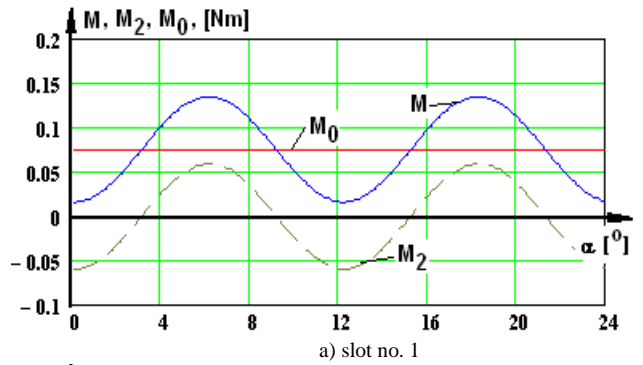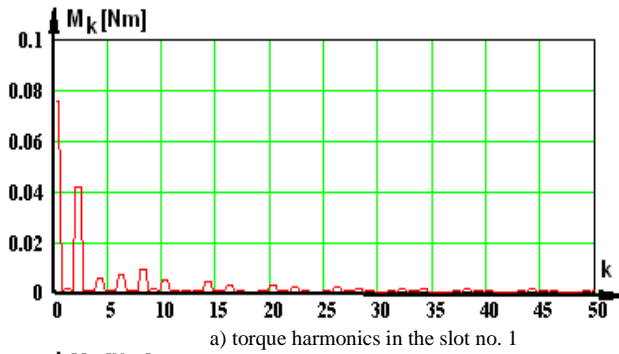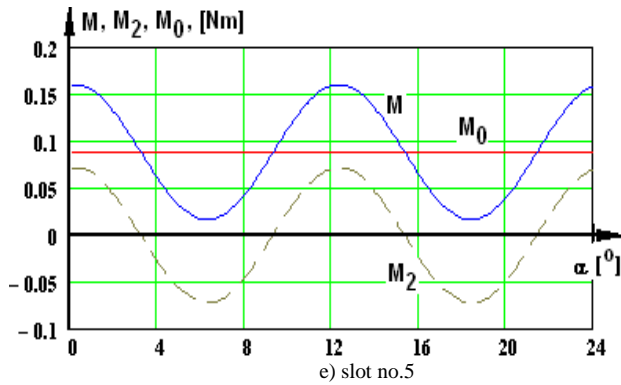
d) slot no. 4

e) slot no.5

Fig.12. Variation curves for a pole pair, for the continuous component, the second order harmonic and their sum.

TABLE III. Analysis of slot torque for a period

Slot no.	Torques			Distortion factor
	Average value M_{med} [Nm]	Important harmonics M_k [Nm]		K_{dis} [%]
1	0.075	M_2=0.042	M_8=0.009	51.03
2	0.048	M_2=0.067	M_6=0.018	83.59
3	0.019	M_2=0.077	M_4=0.022	97.63
4	0.035	M_2=0.029	M_6=0.008	66.32
5	0.088	M_2=0.051	M_4=0.026	56.92

CONCLUSIONS

The research carried out has aimed at analyzing the causes which produce total torque oscillations, in the most favourable case, meaning six-pulse supply, direct sequence of phases and $\gamma = 294^o$ – control angle of the a - phase current.

The simulations presented before and the results filled in the Table III show that we have five classes of slots relatively to the magnitude of the torque provided and the fact that all slots are active, meaning the average torque developed is in the rotation sense. The torques computed for slots classes are within the minimum limit, M_{min}= 0.029 Nm, and the maximum one, M_{max}= 0.077 Nm.

The slots belonging to the classes I (six) and V (three) have an accepted value of the average torque and a small distortion factor, $k_{disMcr.I}$ =51.03% and $k_{disMcr.V}$=56,92%.

The slots belonging to the classes II (three) and III (three) have high average torques, but they also have a high distortion factor, $k_{disMcr.II}$ =83.59% and $k_{disMcr.V}$=97.63%.

The slots belonging to the class IV (four) produce the smallest torque, with a distortion factor $k_{disMcr.IV}$=66.32%.

This is the explanation for high torque oscillations which occur in brushless direct current motors. An almost constant torque cannot be obtained with this motor, but it is possible to be close to fulfilling this requirement.

The torque variation for a pole pair is a major drawback and it is explained by an imperfect commutation of the phase currents and by the position occupied by slots in the inductor magnetic field.

The high inertia moment of the rotor and the high speed decrease the speed oscillations caused by the torque variations. A speed reaction loop and a performant control system can reduce substantially the torque oscillations at low speed.

REFERENCES

[1] C. Bianchini, F. Immovilli, E. Lorenzani, A. Bellini, M. Davoli, "Review of Design Solutions for Internal Permanent Magnet Machines Cogging Torque Reduction", *IEEE Transactions on Magnetics*, Vol. 48, No.10, 2012, pp 2685-2693.

[2] J. Cros, P. Viarouge, R. Carlson, L.V. Dokonal, "Comparison of brushless DC motors with concentrated windings and segmented stator", *ICEM 2004*, Krakow, Poland, 2004

[3] L. Dosiek, P. Pillay, "Cogging Torque Reduction in Permanent Magnet Machines", *IEEE Trans. On Industry Applications*, Vol. 43, No. 6, 2007, pp 1565-1571.

[4] W. Fei, P.C.K. Luk, "A New Technique of cogging Torque Suppression in Direct-Drive Permanent-Magnet Brushless Machines", *IEEE Trans. on Industry Applications*, Vol 46, No. 4, 2010, pp. 1332-1340.

[5] http://www.bicicleteelectrice.com/2015/06/bicicleta-electrica-zt-08.html

[6] [3] http://www.keewayromania.ro/ro/

[7] [4] http://www.bizoo.ro/firma/nogal/vanzare/6890815/tricicleta-adulti-electrica-zt02

[8] https://sistemeortopedice.ro/scuter-electric/136-scuter-electric-vantage-x.html

[9] M.S. Islam, S. Mir, T. Sebastian, "Issues in reducing the cogging torque of mass-produced permanent magnet brushless DC motor", *IEEE Trans. on Industry Applications*, Vol. 40, No. 3, 2004, pp.813 – 820.

[10] J. Kaňuch, Z. Ferková, "Design and simulation of disk stepper motor with permanent magnets", *Archives of Electrical Engineering*, Vol. 62, No. 2, 2013, pp. 281-288.

[11] T. Koch, A. Binder, "Permanent magnet machines with fractional slot winding for electric traction", ICEM 2002, Brugge, 2002.

[12] *** Catalog ICPE Bucharest, Al-Ni-Co and Nd-Fe-B sintherised magnets–magnetic features.

[13] http://www.magneticsmagazine.com/main/ channels/ magnetic assemblies/ passive-magnetic-bearing-prototype-testing-results/.

[14] W.C. Chi, M.Y. Cheng, C.H. Chen, "Position-sensorless method for electric braking commutation of brushless DC machines", *IET Electric Power Applications*, Vol.7, Issue 9, 2013, pp.701-713.

[15] M. Miyamasu, K. Akatsu, "Efficiency Comparison between Brushless DC Motor and Brushless AC Motor Considering Driving Method and Machine Design", *37th Annual Conference of the IEEE Industrial-Electronics-Society IECON 2011*, pp.1830-1835.

[16] M. Ancău, L. Nistor, "Optimization Numerical Techniques in Computer-aided Design", *Bucharest, Technical Publishing House,* 1996.

[17] T. Tudorache, L. Melcescu, M. Popescu, "Methods for Cogging Torque Reduction of Directly Driven PM Wind Generators", *12th International Conference on Optimization of Electrical and Electronic Equipment*, OPTIM, 2010.

Y.L. Zhang, W. Hua, M. Cheng, G. Zhang, X.F. Fu, "Static Characteristic of a Novel Stator Surface-Mounted Permanent Magnet Machine for Brushless DC Drives", *38th Annual Conference on IEEE-Industrial-Electronics-Society (IECON 2012)*, 2012, pp.4139-4144.